BioCapt® Single-Use

Aktiver Luftkeimsammler

Testfertiger, aktiver Ersatz für Sedimentationsplatten

- Kontinuierliche Luftprobenahme und Überwachung
- Testfertiger Ersatz für Sedimentationsplatten
- Weniger Handhabungsschritte und weniger falsch-positive Untersuchungen
- Für den mobilen oder remote Einsatz
- Auswahl verschiedener Agarformulierungen und Flussraten
- Erfüllt ISO 14698-1 und den erwarteten EU-GMP-Annex 1 Einweg-Anforderungen
- Verwendung mit aktiven Luftkeimsammler-Instrumenten für eine vollständig validierte Lösung

Mehr erfahren

PARTICLE MEASURING SYSTEMS®
a spectris company

Kontaktieren Sie uns für mehr Informationen:

www.pmeasuring.de
T: +49 351 8896 3850
E: pmsgermany@pmeasuring.com

Received: 16 December 2022 | Revised: 11 February 2023 | Accepted: 11 February 2023

DOI: 10.1002/bit.28354

ARTICLE

BIOTECHNOLOGY AND BIOENGINEERING WILEY

Reaction intensification for biocatalytic production of polyphenolic natural product di-*C*-β-glucosides

Tuo Li[1,2] | Annika J. E. Borg[1,2] | Leo Krammer[3] | Rolf Breinbauer[3] | Bernd Nidetzky[1,2]

[1]Institute of Biotechnology and Biochemical Engineering, Graz University of Technology, NAWI Graz, Graz, Austria

[2]Austrian Centre of Industrial Biotechnology (acib), Graz, Austria

[3]Institute of Organic Chemistry, Graz University of Technology, NAWI Graz, Graz, Austria

Correspondence
Bernd Nidetzky, Institute of Biotechnology and Biochemical Engineering, Graz University of Technology, NAWI Graz, Petersgasse 12/1, 8010 Graz, Austria.
Email: bernd.nidetzky@tugraz.at

Funding information
Österreichische Forschungsförderungsgesellschaft

Abstract

Polyphenolic aglycones featuring two sugars individually attached via *C*-glycosidic linkage (di-*C*-glycosides) represent a rare class of plant natural products with unique physicochemical properties and biological activities. Natural scarcity of such di-*C*-glycosides limits their use-inspired exploration as pharmaceutical ingredients. Here, we show a biocatalytic process technology for reaction-intensified production of the di-*C*-β-glucosides of two representative phenol substrates, phloretin (a natural flavonoid) and phenyl-trihydroxyacetophenone (a phenolic synthon for synthesis), from sucrose. The synthesis proceeds via an iterative two-fold *C*-glycosylation of the respective aglycone, supplied as inclusion complex with 2-hydroxypropyl β-cyclodextrin for enhanced water solubility of up to 50 mmol/L, catalyzed by a kumquat di-*C*-glycosyltransferase (di-CGT), and it uses UDP-Glc provided in situ from sucrose by a soybean sucrose synthase, with catalytic amounts (≤3 mol%) of UDP added. Time course analysis reveals the second *C*-glycosylation as rate-limiting (0.4–0.5 mmol/L/min) for the di-*C*-glucoside production. With internal supply from sucrose keeping the UDP-Glc at a constant steady-state concentration (≥50% of the UDP added) during the reaction, the di-*C*-glycosylation is driven to completion (≥95% yield). Contrary to the mono-*C*-glucoside intermediate which is stable, the di-*C*-glucoside requires the addition of reducing agent (10 mmol/L 2-mercaptoethanol) to prevent its decomposition during the synthesis. Both di-*C*-glucosides are isolated from the reaction mixtures in excellent purity (≥95%), and their expected structures are confirmed by NMR. Collectively, this study demonstrates efficient glycosyltransferase cascade reaction for flexible use in natural product di-*C*-β-glucoside synthesis from expedient substrates.

KEYWORDS

cascade reaction, di-*C*-glycosyltransferase, natural product di-*C*-glucoside, polyphenol, process intensification

Abbreviations: CGTs, *C*-glycosyltransferases; *Fc*CGT, *C*-glycosyltransferase from kumquat (*Fortunella crassifolia*); *Gm*SuSy, sucrose synthase from soybean (*Glycine max*); HPCD, 2-hydroxypropyl-β-cyclodextrin; PTHAP, 2-phenyl-2′,4′,6′-trihydroxyacetophenone; UDP, uridine-5′-diphosphate; UDP-Glc, UDP-glucose; UMP, uridine-5′-monophosphate; TLC, thin-layer chromatography.

Tuo Li and Annika J. E. Borg are equally contributing first authors.

1 | INTRODUCTION

Polyphenols (e.g., flavonoids, anthrones) are a large class of natural products widely distributed in plants (phytochemicals) (Abbas et al., 2016; Durazzo et al., 2019; Rasouli et al., 2017). They are generally considered important in a healthy human diet and contribute to the efficacy of traditional medicines (Luo et al., 2021; Mithul Aravind et al., 2021; Shakoor et al., 2021; C. Sun, Zhao, et al., 2020). Polyphenol biosynthesis often involves the late-stage attachment of one or more sugar residues to the aglycone core structure (Li et al., 2021; Thuan & Sohng, 2013). A distinct natural motif of polyphenol glycosylation is that of the di-*C*-glycoside. This involves two sugars individually linked to the same benzene ring of the polyphenol via a *C*-glycosidic bond (Kitamura et al., 2018; Y. Q. Zhang et al., 2022). The type of glycosylation most often used is that of *C*-β-D-glucosyl (Figure 1) (C. F. Liu, 2022; Y. Q. Zhang et al., 2022).

The di-*C*-glycosides of polyphenols have attracted attention for the unique chemical properties and bioactivities they can offer (Xiao et al., 2016; Zeng et al., 2013). Generally, the *C*-glycosidic linkage is resistant to hydrolysis (Putkaradze et al., 2021; Tegl & Nidetzky, 2020; Y. Q. Zhang et al., 2022). The *C*-glycosyl substituents further activate the aromatic ring of the polyphenol to readily donate an electron towards antioxidant function (Kanamori et al., 2018; Mannem et al., 2020; Marrelli et al., 2014; Materska, 2014; Wen et al., 2017; Xiao et al., 2014; Xie et al., 2020). Contrariwise, an *O*-glycosyl substituent can destroy the antioxidant properties of the polyphenol, depending on the glycosylation site used (Xiao, 2015). The polyphenol bioavailability linked to its solubility in water is strongly altered through the appendage of the di-*C*-β-glucoside motif (Sato et al., 2020). Although various polyphenol di-*C*-β-glucosides have been reported from different plant species (Oualid & M. S. Silva, 2012), their natural abundance is not sufficient for large-scale isolation from the immediate source (Shie et al., 2010). Low availability often limits even the systematic early-stage assessment of their biological activity as basis for the development of future uses (Kaur & Kaur, 2014). Synthetic routes for the facile installment of the di-*C*-β-glucoside motif on different polyphenol core structures are therefore highly desirable. Here we show a biocatalytic process technology for an efficient and flexible di-*C*-β-glucoside production.

The biosynthesis of di-*C*-β-glucosides involves a special subclass of sugar nucleotide-dependent (Leloir) glycosyltransferases (GTs) (He et al., 2022). The enzymes, here referred to as CGTs, use uridine-5′-diphosphate (UDP)-glucose for site-selective *C*-β-glycosylation of the polyphenol acceptor substrate (Figure 1) (Chong et al., 2022; Dai et al., 2021; Gao et al., 2022; Putkaradze et al., 2021; Tegl & Nidetzky, 2020; Y. Q. Zhang et al., 2022). The iterative two-fold

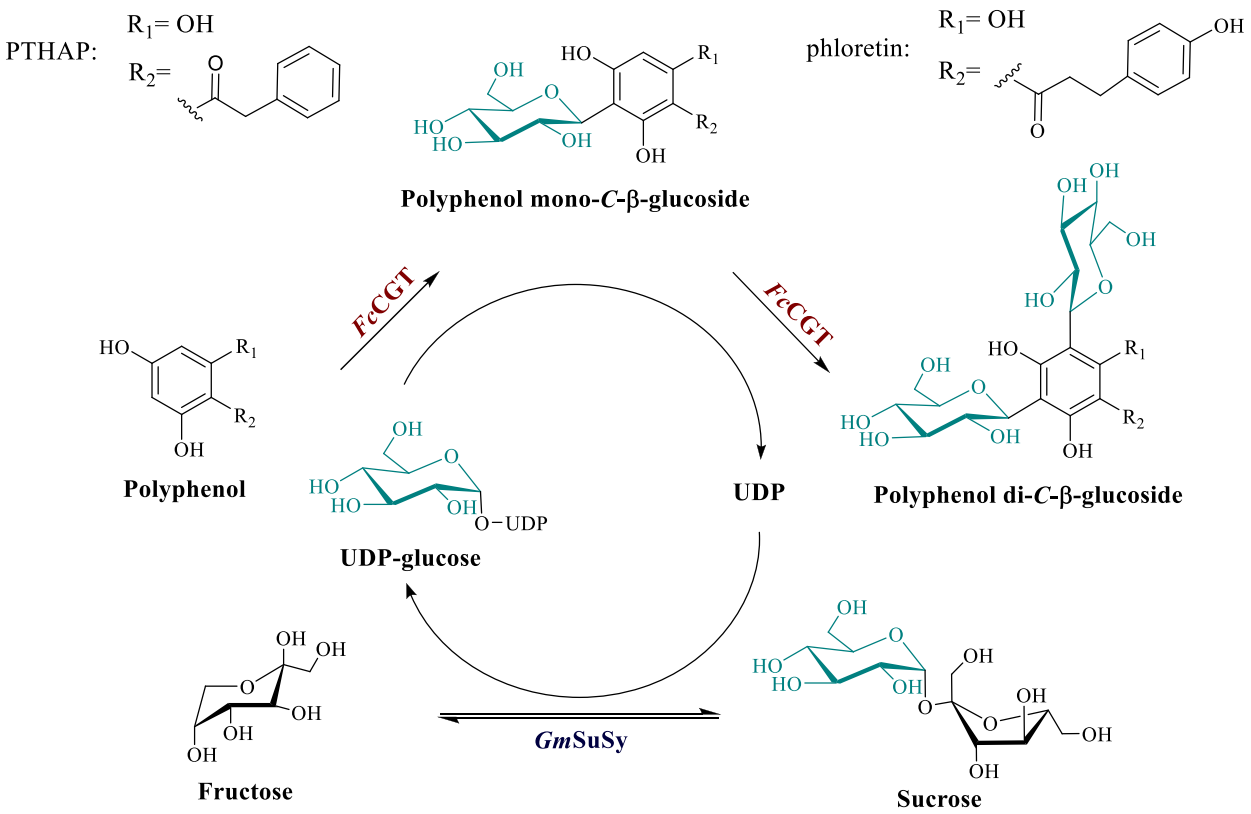

FIGURE 1 Reaction scheme for the synthesis of a polyphenol-di-*C*-β-glucoside by *C*-glycosyltransferase *Fc*CGT, coupled with UDP-Glc production and regeneration by a sucrose synthase *Gm*SuSy. PTHAP, 2-phenyl-2′,4′,6′-trihydroxyacetophenone; UDP, uridine-5′-diphosphate; UDP-Glc, UDP-glucose.

glycosylation leading to the di-*C*-β-glucosides may arise from the coordinated action of separate CGTs (Feng et al., 2021; Y. Sun, Chen, et al., 2020; Z. L. Wang et al., 2020), but as recent works have shown, a single dual-specific di-CGT can also be sufficient to form the fully di-glycosylated product. Within a rapidly growing number (≥67) of plant CGTs isolated and characterized (Bao et al., 2022; Y. Q. Zhang et al., 2022), only a few enzymes manage the difficult task of iterative glycosylation to release the di-*C*-glucoside product: *Fc*CGT, *Fortunella crassifolia* and *Cu*CGT, *Citrus unshiu* (Ito et al., 2017); *Mi*CGTb, *Mangifera indica* (Chen, Fan, et al., 2018); *Gg*CGT, *Glycyrrhiza glabra* (M. Zhang et al., 2020); *Dca*CGT, *Dendrobium catenatum* (Ren et al., 2020); *Ab*CGT, *Aloe barbadensis* (Xie et al., 2020); *Aa*CGT, *Anemarrhena asphodeloides* (Huang et al., 2022), and *Ad*CGT, *Angelica decursiva* (Z. Wang et al., 2022). Compared to CGTs performing only a single *C*-glycosylation, a relatively open and spacious acceptor substrate-binding pocket appears to be requirement of the protein structure for di-CGT activity (Chen, Fan, et al., 2018; M. Zhang et al., 2020). The known di-CGTs were analyzed for substrate scope in diversity-oriented small-scale syntheses done as part of their characterization (Chen, Fan, et al., 2018; Ito et al., 2017; M. Zhang et al., 2020). While the enzymes hold promise as selective catalysts of the di-*C*-β-glucoside formation, it remained to be shown that di-CGTs are applicable to synthetic glycosylation reactions that fulfill the requirement of being amenable to a biocatalytic production at larger scale in principle. In particular, glycosylation from substrate more expedient than UDP-Glc and reaction intensification to obtain the di-*C*-β-glucoside as single product in high yield and concentration were important tasks for development in the current study. Indeed, earlier attempts (Chen, Chen, et al., 2018) to synthesize di-*C*-β-glucosides in CGT-expressing *E. coli* cells gave the target product in relatively low yield (≤2.8%, based on the limiting acceptor concentration) and rather insufficient amount (≤0.04 g/L). Here, we show the *Fc*CGT for an efficient synthesis of the di-*C*-β-glucoside of phloretin, a dihydrochalcone of the flavonoid class and representative polyphenol of plant origin (Behzad et al., 2017). To become truly efficient, the enzymatic di-glycosylation required intensification (≥100-fold) along three lines of reaction engineering: (1) cascade reaction development for an overall glycosylation that proceeds fully to the di-glycosylated product and uses an expedient substrate, here sucrose (Figure 1); (2) aglycone solubility enhancement through means compatible with enzyme activity and stability, here encapsulation in 2-hydroxypropyl-β-cyclodextrin (HPCD; H. Liu & Nidetzky, 2021; H. Liu et al., 2021; Schmölzer et al., 2018); and (3) di-*C*-β-glucoside product stabilization during the reaction, as discovered in the current study. A biocatalytic process technology for the selective production of the phloretin-3′,5′-di-*C*-β-glucoside in high reaction yield (≥95%), concentration (~40 mM; 24 g/L), and good recovery rate (≥80%) as a high-purity product (≥98%) is shown. Replication potential of the technology is demonstrated for production of the 3′,5′-di-*C*-β-glucoside of 2-phenyl-2′,4′,6′-trihydroxyacetophenone (PTHAP; Figure 1) which is equally efficient as the phloretin di-glycosylation by the criterions used.

2 | MATERIALS AND METHODS

2.1 | Materials

Phloretin (>98%), HPCD (>96%), UDP (>97%) and UDP-Glc (>98%) were from Carbosynth (Compton, UK). PTHAP (>97%) was from Sigma Aldrich (Vienna, Austria). Sucrose (>99%), and 2-mercaptoethanol (>99%) were from Roth (Karlsruhe, Germany). Standard of nothofagin (phloretin-3′-*C*-β-D-glucoside; >99%) was obtained from a previous study using enzymatic synthesis (Schmölzer et al., 2018). All other reagents and chemicals were of highest available purity and purchased from Sigma Aldrich/Fluka (Vienna, Austria), Roth (Karlsruhe, Germa), or Merck (Vienna, Austria).

2.2 | Encapsulation of acceptor substrates by HPCD

HPCD inclusion complexes of phloretin were prepared according to a protocol from literature (Schmölzer et al., 2018), with the molar ratio of 1.25:1 for HPCD to phloretin. The PTHAP inclusion complexation was performed with a modified protocol from that described in the literature (Schmölzer et al., 2018), using the molar ratio of 2:1 for HPCD to PTHAP. The actual concentrations of encapsulated acceptor substrates were determined based on calibration curves (Supporting Information: Figure S1). Full details of the inclusion complex formation and concentration measurements are given in the Supporting Information under "Encapsulation of acceptor substrates by HPCD".

2.3 | Enzyme production

The codon-optimized synthetic gene of *Fc*CGT (Gene UGT708G1; Supporting Information: Figure S2) in a pET-28a expression vector was purchased from GenScript (Germany) and transformed into *E. coli* BL21(DE3) cells. *Fc*CGT was expressed in Terrific Broth (TB) medium containing 4% (v/v) glycerol and purified utilizing an N-terminal 6xHis-tag. The size and purity of *Fc*CGT were confirmed by SDS-PAGE (Supporting Information: Figure S3A). The sucrose synthase from soybean (*Glycine max*; *Gm*SuSy) was produced by expression in *E. coli* BL21-Gold (DE3) cells and purified utilizing an N-terminal Strep-Tag II. The size and purity of *Gm*SuSy were confirmed by SDS-PAGE (Supporting Information: Figure S3B). Full details of the expression and purification conditions used are given in the Supporting Information under "Enzyme production".

2.4 | Enzyme activity assays

The specific activity of *Fc*CGT towards free and HPCD-encapsulated phloretin/PTHAP was determined in an enzymatic assay containing 1.0 mM acceptor substrate and 5.0 mM UDP-Glc. The initial rates for

mono- and di-*C*-glycosylation were calculated from the corresponding time courses (Supporting Information: Figures S4 and S5). The activity of *Gm*SuSy on UDP (2.0 mM) was determined from a time course (Supporting Information: Figure S6) of the reaction with 500 mM sucrose. Full details of the activity assays are provided in the Supporting Information under "Enzyme activity assays".

2.5 | Optimization of parameters for reaction intensification

2.5.1 | Single-enzyme reactions with *Fc*CGT

Due to low stability of the di-*C*-glucosides, the reactions (100 µL) of phloretin were optimized for the pH, buffer salt, and presence of reducing agents/antioxidants. All the reactions were performed with 1.0 mM acceptor substrate (DMSO, 2%), 5.0 mM UDP-Glc, and 0.1 mg/mL (1.94 µM) *Fc*CGT at 30°C. For the buffer salt investigation, 50 mM Tris or K_2HPO_4 was tested at pH 8.0. For the pH optimization, K_2HPO_4 buffer at pH 6.0–8.0 was used. For the reactions with reducing agents/antioxidants, K_2HPO_4 buffer (pH 8.0) was supplemented with tris(2-carboxyethyl)phosphine (TCEP, 2.0 mM), and/or ascorbic acid (1.0 mM), or 2-mercaptoethnol (12.5 mM). The reactions were quenched and analyzed on high-performance liquid chromatography (HPLC) for the UDP and glucoside product formation as described in the Supporting Information under "Enzyme activity assays."

2.5.2 | Cascade reactions with *Fc*CGT and *Gm*SuSy on HPCD-encapsulated acceptors

The reactions were performed in HEPES (50 mM) buffer containing KCl (50 mM), $MgCl_2$ (13 mM), and BSA (0.13%) in the final volume of 100 µL. The buffer composition was based on our earlier work on GT cascade reactions (e.g., H. Liu & Nidetzky, 2021; Schmölzer et al., 2018). The BSA is added as a general enzyme stabilizer. GTs can inactivate through different mechanisms (Teze et al., 2022). The HPCD-encapsulated acceptor (phloretin, 10–40 mM; PTHAP, 30–50 mM), 2-mercaptoethanol (10 mM), and sucrose (500 mM) were dissolved in the reaction buffer, followed by the addition of *Fc*CGT (1.0–6.0 mg/mL) and *Gm*SuSy (0.5–3.0 mg/mL). The reactions were started with UDP (0.5–3.0 mM) addition. In the 50 mM phloretin reaction with batch-addition of the enzymes, 2.0 mg/mL *Fc*CGT and 1.0 mg/mL *Gm*SuSy were supplied at the start, and 1.5 mg/mL *Fc*CGT and 0.8 mg/mL *Gm*SuSy after 4 h of reaction. The reactions were performed at desired temperature (30–45°C) and pH (6.5–7.0) conditions. For all the reactions running longer than 8 h, a second batch of 2-mercaptoethanol (10 mM) was supplemented at 8 h. The sampling and HPLC analysis (Figures 3–5 and Supporting Information: Figures S7–S15) were carried out as described in the Supporting Information under "Enzyme activity assays".

2.6 | Di-C-β-glucoside production and isolation

2.6.1 | Phloretin-3′,5′-di-C-β-glucoside

The reactions (4 × 1.0 mL) were carried out in 2 mL Eppendorf tubes under the following conditions: 30 mM phloretin-HPCD complex, 500 mM sucrose, 0.50 mM UDP, 5.0 mg/mL (97 µM) *Fc*CGT, 2.0 mg/mL (22 µM) *Gm*SuSy, and 10 mM 2-mercaptoethanol in 50 mM HEPES buffer (pH 6.5, containing 50 mM KCl, 13 mM $MgCl_2$, and 0.13% BSA) at 45°C. The reactions were sampled at desired time points by quenching 5 µL of reaction mixture with 50 µL methanol and 45 µL HCl (final concentration 10 mM), and the samples were subjected to HPLC and thin-layer chromatography (TLC) analysis. After reaching a full conversion to the di-*C*-glucoside (Supporting Information: Figure S16), the reactions were quenched by freezing in liquid nitrogen and stored at −20°C. The thawed reaction mixtures were centrifuged (21130*g*, 4°C, 30 min) and the supernatant subjected to purification by anion exchange- and size-exclusion chromatography (Supporting Information: Figures S17 and S18) based on literature protocols (Lemmerer et al., 2016; Schmölzer et al., 2018). Aliquots (80 µL) of the thawed reaction mixture were additionally subjected to liquid–liquid extraction with organic solvents (80 µL; 1-butanol, 1-octanol, diethyl ether, ethyl acetate, dichloromethane). The extraction was repeated three times, organic- and aqueous phases collected and analyzed on TLC (Supporting Information: Figure S19A). Up-scaled extraction with 1-butanol: Reaction mixture (0.7 mL) was extracted with 1-butanol (3 × 3.0 mL), the organic phases combined and solvent removed under reduced pressure on a Laborota 4000 rotary evaporator (Heidolph) at 40°C. The solid material was dissolved in acetone (2.0 mL) followed by addition of deionized water (2.0 mL) and the samples analyzed by TLC (Supporting Information: Figure S19B). For the final product isolation via TLC, the remaining reaction mixture (1.20 mL) was loaded onto silica plates (20 cm × 20 cm, layer thickness 2 mm; Merck). The target product was isolated from the TLC plate (Supporting Information: Figure S20) as described in the Supporting Information under "Di-*C*-β-glucoside product isolation". The purity and identity of phloretin-3′,5′-di-*C*-β-glucoside were analyzed on HPLC (Supporting Information: Figure S21) and nuclear magnetic resonance (NMR) (Supporting Information: Figure S22).

2.6.2 | PTHAP-3′,5′-di-C-β-glucoside

The reactions (3 × 1.0 mL) were performed and analyzed as described under "Phloretin-3′,5′-di-*C*-β-glucoside," except that PTHAP-HPCD complex (30 mM) was used. When PTHAP was fully converted to the corresponding di-*C*-glucoside (Supporting Information: Figure S23), the reaction mixtures were handled as described under phloretin-3′,5′-di-*C*-β-glucoside production. A part of the supernatant (1.8 mL) was subjected to product isolation via silica column chromatography using a combination of C18 and silica 60 columns. Full details of the column chromatographic procedure are given in the Supporting

Information under "Di-*C*-β-glucoside product isolation". The purity and identity of PTHAP-3′,5′-di-*C*-β-glucoside were confirmed on HPLC-MS (Supporting Information: Figure S24) and NMR (Supporting Information: Figure S25).

2.7 | Analytical methods

2.7.1 | HPLC-UV

UDP-Glc and UDP were separated with Shimadzu Prominence HPLC-UV system (Shimadzu) on a Kinetex C18 column (5 µm, 100 Å, 50 × 4.6 mm) using an isocratic method (2.0 mL/min) with 5% acetonitrile (MeCN) and 95% tetrabutylammonium bromide (TBAB) buffer (40 mM TBAB, 20 mM K_2HPO_4/KH_2PO_4, pH 5.9) as the mobile phase. UDP-Glc and UDP were detected by UV at 262 nm wavelength. Acceptor substrates and glucoside products were separated with Agilent 1200 Series HPLC-UV system on a Kinetex C18 column (5 µm, 100 Å, 150 × 4.6 mm) using a gradient method (1.0 mL/min) of water and MeCN (each containing 0.1% (v/v) formic acid) as the mobile phase. Gradient: 20%–75% MeCN in 7 min, 75%–20% MeCN in 2 min, total time 9 min. The acceptor substrates and glucoside products were detected by UV at 288 nm wavelength. The details of HPLC-MS used in the analysis of PTHAP-3′,5′-di-*C*-β-glucoside are given in the Supporting Information.

2.7.2 | TLC, HPLC-UV/MS, and NMR

Full details of the methods are provided in the Supporting Information under "Analytical methods—TLC, HPLC-UV/MS, and NMR".

3 | RESULTS AND DISCUSSION

3.1 | Biocatalytic reaction system

The *C*-glycosyltransferase *Fc*CGT was used for its reported activity of di-β-*C*-glycosylation of both phloretin and PTHAP (Ito et al., 2017). Among the various CGTs reported in the literature, *Fc*CGT appeared to be a promising candidate enzyme to be used in a study of reaction intensification. The *Fc*CGT was isolated from *Escherichia coli* expression culture at 3.3 mg protein/L (Supporting Information: Figure S3). Expression in LB medium according to literature (Ito et al., 2017) did not give soluble protein. Soluble expression was achieved in TB medium supplemented with 4% of glycerol, with less IPTG (0.2 mM instead of 0.4 mM) and lower expression temperature (18°C instead of 22°C) used. A substantial fraction of the enzyme (~60%; estimated from Supporting Information: Figure S3) was however still insoluble. The purified *Fc*CGT (see the Supporting Information Methods for the procedure used) had a specific activity (mono-*C*-glycosylation of phloretin from UDP-Glc; Supporting Information: Figure S4A) of 3.02 U/mg (±1%; $N = 2$). The specific activity for the further *C*-glycosylation of nothofagin (Supporting Information: Figure S4A) was ~7.4-fold lower at 0.41 U/mg (±10%; $N = 2$). Earlier work on *Fc*CGT described the enzyme as more active towards nothofagin (3.57 U/mg) than phloretin (2.04 U/mg) (Ito et al., 2017). In other di-glycosylating *O*- or *C*-glycosyltransferases, however, the second glycosylation was slower considerably than the first (Chen, Fan, et al., 2018; M. Zhang et al., 2020). Using PTHAP as the acceptor, *Fc*CGT had a specific activity of 3.25 U/mg (±6%; $N = 2$) and 0.48 U/mg (±7%; $N = 2$) for the first and the second *C*-glycosylation, respectively (Supporting Information: Figure S5A). Interestingly, the specific activities for PTHAP di-*C*-glycosylation are in accordance with literature on *Fc*CGT (Ito et al., 2017). Both acceptor substrates used have limited solubility in the reaction buffer (2% DMSO co-solvent) at the relevant temperature of 30–45°C (phloretin: ~1.0 mM; PTHAP: ~6.0 mM). Considering the process intensification goal of the current study, inclusion complexation with HPCD (Figure 1) was employed for their solubility enhancement. Earlier evidence on the biocatalytic production of nothofagin strongly suggested the HPCD-based approach be used, not only for its efficiency at phloretin solubilization (≥100 mM) but also for its excellent compatibility with activity and stability of the enzymes (CGT from *Oryza sativa*; SuSy from *Glycine max*) (H. Liu et al., 2021; Schmölzer et al., 2018). While the phloretin–HPCD complex (~150 mM phloretin solubilized) was obtained as previously reported, preparation of the PTHAP–HPCD complex required a guest molecule-specific adaptation of the conditions whereby in particular the molar ratio HPCD/acceptor was increased to 2.00, instead of 1.25 for phloretin (see the Materials and Methods section for the full procedure). The soluble PTHAP concentration was thus enhanced ~4-fold from 24 mM (14 g/L) in the standard complexation to ~100 mM (57 g/L) in the optimized procedure. With both acceptor substrates, the basal solubility in water was increased by two orders of magnitude as a result of complex formation with the HPCD.

Standard enzyme assays performed with the acceptor–HPCD complex instead of the free acceptor gave specific activities of 1.82 U/mg (±8%; $N = 2$) and 0.09 U/mg (±10%; $N = 2$) for the first and second *C*-glycosylation on the phloretin (Supporting Information: Figure S4B). Compared to the free phloretin, the inclusion complex showed lower apparent activity in particular in the second *C*-glycosylation (4.6-fold decrease). Interestingly, therefore, the *Fc*CGT exhibited even higher apparent activity towards PTHAP-HPCD than free PTHAP, with specific activities of 3.92 U/mg (±3%; $N = 2$) and 0.65 U/mg (±3%; $N = 2$) determined for the first and second *C*-glycosylation, respectively (Supporting Information: Figure S5B). Phloretin and PTHAP may differ in various ways regarding their inclusion complexes with HPCD in the nonglycosylated as well as the mono-*C*-glycosylated form (e.g., molecular orientation and dynamic equilibrium of the host–guest molecule interaction), as generally suggested by literature on complexation by cyclodextrins (Cesari et al., 2020; Fang & Bhandari, 2010; Gratieri et al., 2020; Kellici et al., 2016; Zheng et al., 2005) While interesting, an exploration into the molecular origins of the observed effects was not within the scope of the current study. With both acceptors, however, feasibility of inclusion complexation for *Fc*CGT

substrate solubility enhancement was demonstrated in view of the intended di-*C*-glycoside synthesis.

3.2 | Product stability during the enzymatic reaction

Using initially a low concentration of the acceptor (1.0 mM) in free form or as the HPCD complex, we monitored the time course of *C*-glycoside formation in the *Fc*CGT reaction, now aiming at full conversion into the doubly *C*-glycosylated product. Unexpectedly, we discovered the di-*C*-β-glucoside to decompose rapidly in the reaction, irrespective of whether phloretin or PTHAP was used (Figure 2a). The corresponding mono-*C*-β-glucoside appeared to be stable. Inclusion complexation of the acceptor substrate did not enhance the stability of the di-*C*-glycoside formed. Analyzing the phloretin-3′,5′-di-*C*-β-glucoside in more detail, we showed that after extended reaction (≥8 h) nearly all of the compound was degraded.

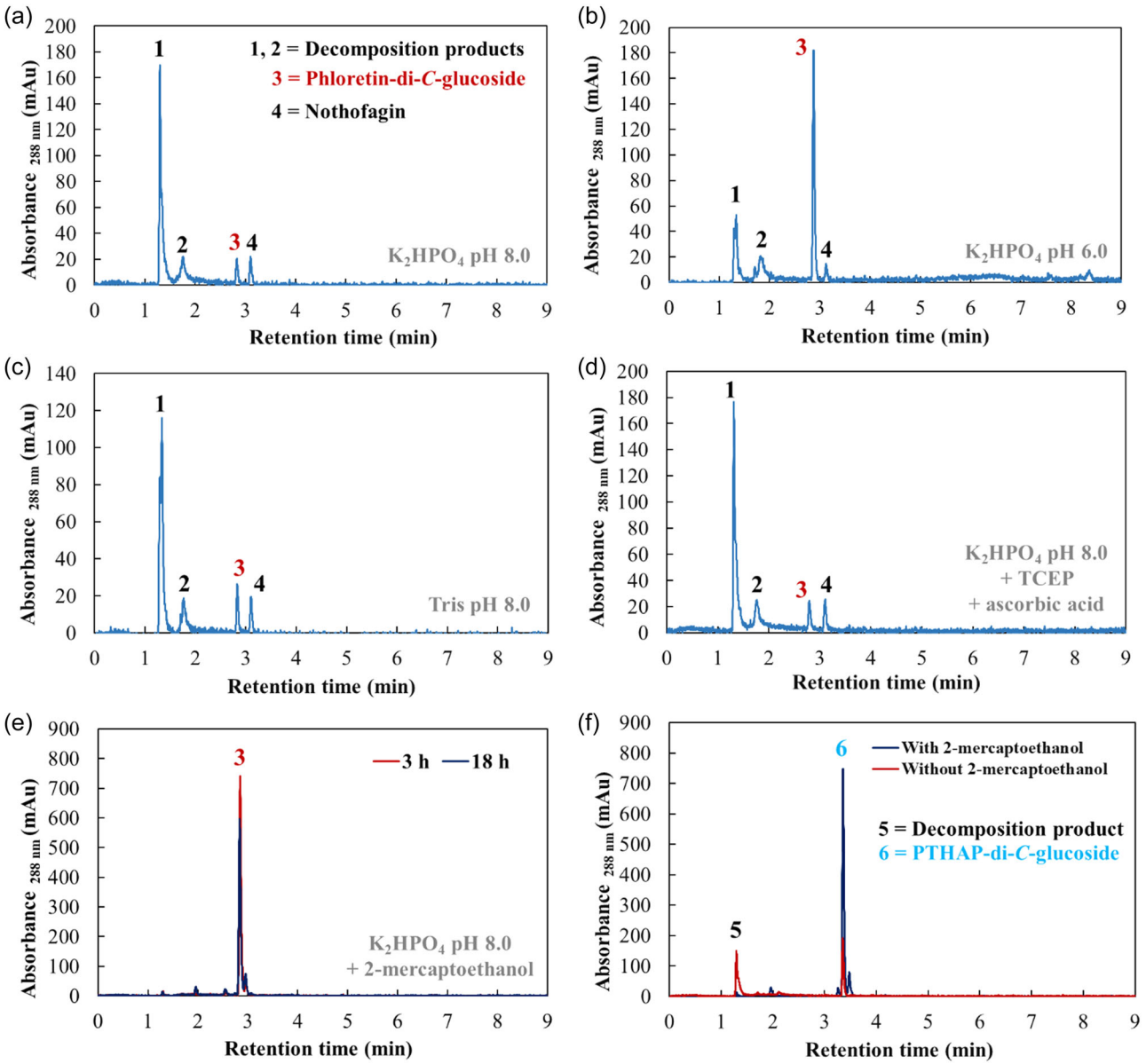

FIGURE 2 Reverse phase high-performance liquid chromatography (HPLC) chromatograms from *Fc*CGT-catalyzed phloretin (a–e) and PTHAP (f) reactions for analyzing the di-*C*-glucoside stability under different reaction conditions. (a) K_2HPO_4 buffer at pH 8.0. (b) K_2HPO_4 buffer at pH 6.0. (c) Tris buffer at pH 8.0. (d) K_2HPO_4 buffer at pH 8.0 with tris(2-carboxyethyl)phosphine (TCEP, 2.0 mM) and ascorbic acid (1.0 mM). (e) Overlay of the HPLC chromatograms after 3 h (red) and 18 h (blue) reaction using K_2HPO_4 buffer at pH 8.0 with 2-mercaptoethanol (12.5 mM). (f) Overlay of the HPLC chromatograms for PTHAP reaction using K_2HPO_4 buffer at pH 8.0 with (blue) or without (red) 2-mercaptoethanol (12.5 mM). Reactions (100 µL) contained 1.0 mM phloretin-DMSO or PTHAP-DMSO, 5.0 mM UDP-Glc, and 0.10 mg/mL (1.94 µM) *Fc*CGT and were carried out at 30°C. The chromatograms for (a–d, f) are from the reactions after 18 h. PTHAP, 2-phenyl-2′, 4′,6′-trihydroxyacetophenone.

pH variation in the range 6.0–8.0 was not effective to achieve stabilization of the di-*C*-glycoside (Figure 2b), nor was exchange of the buffer salt, Tris/K_2HPO_4 (Figure 2c). Considering the decomposition to possibly arise from oxidation events, we examined the effect of reducing agent and antioxidant. The addition of tris(2-carboxyethyl)phosphine (TCEP, 2.0 mM) and L-ascorbic acid (1.0 mM) was not sufficient to prevent the di-*C*-glucoside decomposition (Figure 2d). Finally, 2-mercaptoethanol (12.5 mM) proved highly efficient in preventing the decomposition, and phloretin-3′,5′-di-*C*-β-glucoside was found intact even after 24 h of reaction (Figure 2e). Applying the same conditions to the glycosylation of PTHAP, we show the corresponding 3′,5′-di-*C*-β-glucoside is also stabilized effectively (Figure 2f). Overall, therefore, these results demonstrate that enzymatic synthesis of the di-*C*-β-glucosides of phloretin and PTHAP necessitates stabilization of the product against oxidative decomposition. Low stability is ascribed to the inductive effect of the two *C*-β-glucosyl moieties in the context of a highly substituted, and thus activated, aromatic system. Specific applications of the di-*C*-glycosides that harness their reactivity toward use as pharmacological agents (e.g., antioxidants) or photosensitizers can thus be envisaged (Kanamori et al., 2018; Mannem et al., 2020; Marrelli et al., 2014; Materska, 2014; Wen et al., 2017; Xiao et al., 2014; Xie et al., 2020).

3.3 | Enzyme cascade reaction for di-C-glycosylation of phloretin

For synthesis, we combined the di-*C*-glycosylation of phloretin (HPCD complex) by *Fc*CGT with in situ production of UDP-Glc from sucrose (Figure 1). The sucrose synthase from soybean (*Glycine max*; *Gm*SuSy) was used (Supporting Information: Figure S3B). Except for 2-mercaptoethanol added (10 mM), the basic reaction conditions (Figure 3) were taken from our earlier work on enzyme cascade glycosylation using *Gm*SuSy (H. Liu et al., 2021; Schmölzer et al., 2018). This included UDP used at 0.5 mM and sucrose present in large excess (500 mM). As shown in Figure 3a, phloretin was fully converted into the 3′,5′-di-*C*-β-glucoside. Consistent with the results of the activity assays described earlier, the mono-*C*-β-glucoside (nothofagin) formation rate was much faster (~8-fold) than the di-*C*-glycoside formation rate (Table 1, entry 1). The intermediary nothofagin accumulated to a concentration close (~85%) to that of the initial phloretin concentration (Figure 3a). The distribution of the total UDP added into UDP-Glc and UDP over the reaction time, shown in Figure 3b, suggests proper function of the two-enzyme cascade transformation in terms of usage and provision of the UDP-Glc. It also indicates that the activities of the two enzymes (*Fc*CGT: 1.0 mg/mL, 0.81 U/mL; *Gm*SuSy: 0.5 mg/mL; 0.58 U/mL) were suitably balanced for an efficient recycling of UDP-Glc. During the course of the reaction, UDP-Glc and UDP partially (~10%) decomposed to UMP and uridine (Figure 3c,d). Having demonstrated the biocatalytic cascade reaction for di-*C*-glycoside synthesis in principle, we pursued reaction intensification by way of increase in the phloretin concentration (30–50 mM) along with process parameter optimization (enzyme loading; UDP concentration; temperature; pH). The intensification was aligned to the process tasks of complete conversion of the acceptor substrate into the di-*C*-glycoside product and minimized decomposition of the target product during the reaction. The selected tasks implied a particular focus on fast reaction for selective transformation, while economy of enzyme use, despite its undeniable importance for a comprehensive optimization, had lower priority. A summary of the results is given in Table 1.

Compared to the 10 mM reaction, rate acceleration by increases in enzyme loading and temperature (30°C→45°C) was important at higher phloretin concentrations (e.g., 30 mM; Table 1; entries 2–3) to achieve full conversion. Extension of the reaction time (6 h→24 h) was generally not efficient to enhance the conversion. From a series of experiments performed at 50 mM phloretin (Table 1; entries 4–9), *Fc*CGT stability appeared to be a main factor limiting the conversion obtained. Change in the UDP concentration (0.5–3.0 mM) was ineffective (Table 1, entry 6), suggesting that 0.5–1.0 mM were sufficient. Increase in the *Gm*SuSy loading to change the mass ratio with *Fc*CGT from the usually used 2:1 to 4:3 (Table 1, entry 8) did not affect the phloretin conversion. In all 50 mM reactions, the phloretin was fully converted to nothofagin, but the conversion into the 3′,5′-di-*C*-β-glucoside did not proceed to completion (Supporting Information: Figures S9–S14). The initial rates of release of the mono- and the di-*C*-glycoside were largely unaffected by the change in reaction conditions used (Table 1, entries 4–9). The *C*-glycosylation of the intermediary nothofagin evidently was too slow in the 50 mM reactions to exclude the effect of time-dependent loss of *Fc*CGT activity. Effect noted by Welner and co-workers that family GT1 natural product GTs can show low stability toward their acceptor substrate (Teze et al., 2022), could be relevant here. Evidence that the UDP-Glc/UDP ratio was shifted to a higher value (e.g., 1.0→1.8; Table 1, entries 7 and 8; Supporting Information: Figures S12 and S13) at the point of reaction slowdown further supports the idea of emerging limitation by *Fc*CGT activity. Given the impossibility to convert 50 mM phloretin under all conditions used, we decreased the concentration to 40 mM and performed the reaction at high enzyme loading (total: 9 mg/mL). Full conversion of phloretin was achieved in 4–6 h (Figure 4a,b and Table 1, entry 10), giving a space-time yield of ~10 mM/h for the di-*C*-glycoside product release. The UDP-Glc/UDP ratio was balanced at ~1.2 (Figure 4c and Table 1, entry 10). Significant (~60%) decomposition of UDP and UDP-Glc to uridine and UMP were observed, indicating the high enzyme concentration used to play a role in the donor substrate degradation (Figure 4d).

3.4 | Enzyme cascade reaction for di-C-glycosylation of PTHAP

Using conditions established for the phloretin reaction, we examined enzyme cascade transformation for synthesis of the PTHAP-3′,5′-di-*C*-β-glucoside. Table 1 (entries 11 and 12) shows the results. The conversion of PTHAP (30 mM, HPCD complex) was considerably

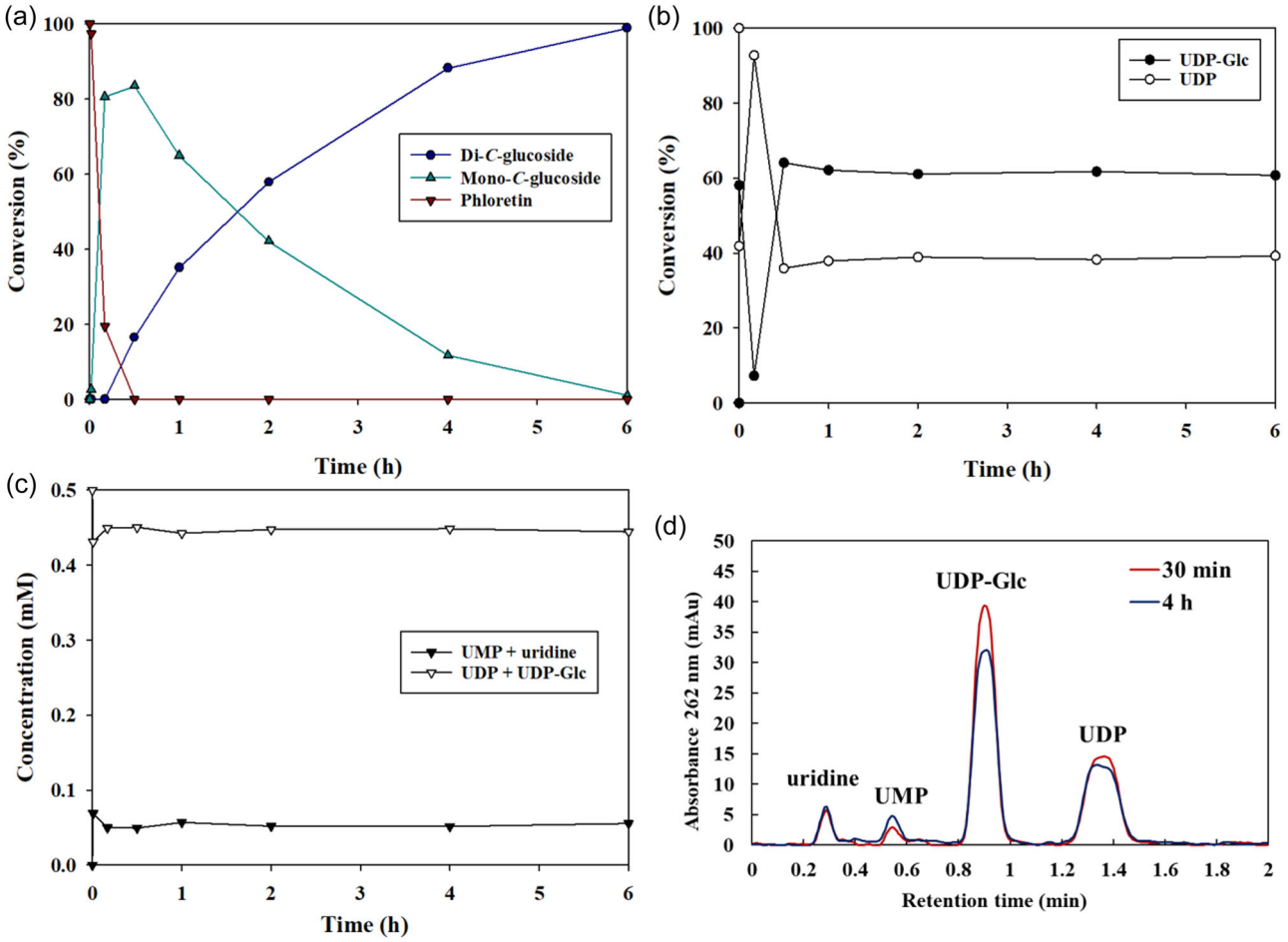

FIGURE 3 Enzyme cascade transformation for di-*C*-glycosylation of phloretin (10 mM; HPCD complex). (a) Time course for phloretin (red triangles), nothofagin (blue circles), and phloretin-3′,5′-di-*C*-β-glucoside (cyan triangles). (b) Time course for UDP (open circles) and UDP-Glc (closed circles). (c) Time course for the summed-up concentrations (mM) of UDP and UDP-Glc (open triangles) and decomposition products uridine and UMP (closed triangles). (d) Overlay of reverse phase HPLC chromatograms for UDP/UDP-Glc/UMP/uridine detection at 30 min (red) and 4 h (blue) reaction time. Besides phloretin, the reaction mixture (100 µL) contained 0.5 mM UDP, 500 mM sucrose, 10 mM 2-mercaptoethanol, 1.0 mg/mL (19.4 µM) *Fc*CGT and 0.50 mg/mL (5.4 µM) *Gm*SuSy in HEPES buffer (50 mM, pH 6.5, including 50 mM KCl, 13 mM $MgCl_2$, 0.13% BSA). Incubation was at 30°C without agitation. HPCD, 2-hydroxypropyl-β-cyclodextrin; UDP, uridine-5′-diphosphate; UDP-Glc, UDP-glucose.

faster (~3-fold) in both glycosylation steps than the comparable conversion of phloretin (Table 1; entries 11 and 3). It proceeded to a quantitative yield of the di-*C*-β-glucoside product (Supporting Information: Figure S15A). The UDP-Glc/UDP ratio in the PTHAP reaction (Supporting Information: Figure S15B and Table 1, entry 11) was notably higher than in the phloretin reaction (Supporting Information: Figure S8 and Table 1, entry 3), indicating a relatively higher rate of UDP-Glc release by the *Gm*SuSy when PTHAP was used. We increased the PTHAP concentration to 50 mM while supplying the same amount of enzyme (Table 1, entry 12) and show full conversion in 24 h (~85% in 8 h; Figure 5a,b). Considering the requirement of full conversion of the acceptor substrate to fulfill the set process tasks, the reaction at 30 mM PTHAP gave a space–time yield (~10 mM/h) substantially higher (5-fold) than that of the reaction at 50 mM PTHAP (~2 mM/h). It seems that the high PTHAP concentration resulted in an inhibition of *Fc*CGT in the second *C*-glycosylation step of the overall transformation (Table 1, entries 11 and 12). Full-fledged optimization of the space–time yield of the di-*C*-glycoside product was beyond the scope of the current study. However, the evidence shown suggests the existence of an optimum substrate concentration for the space–time yield higher than 10 mM and lower than 50 mM.

In the reaction with 50 mM PTHAP, the UDP-Glc donor substrate of *Fc*CGT exhibited interesting dynamics, as shown in Figure 5c. At reaction start, there was an almost instantaneous release of UDP-Glc, corresponding to ~80% of the total UDP present. The UDP-Glc concentration then dropped rapidly to ~50% of the total UDP, reflecting the usage of the UDP-Glc in the fast mono-*C*-glycosylation of the PTHAP. As the second *C*-glycosylation was slower than the first, the UDP-Glc consumption rate decreased and the UDP-Glc concentration increased again to ~50% of the total UDP supplied. Evidence that the initial UDP-Glc concentration was not

TABLE 1 Detailed information of the *Fc*CGT-*Gm*SuSy cascade reactions for the synthesis of di-*C*-glucosides of phloretin and PTHAP.

Entry	Substrate	UDP (mM)	Temp. (°C)	*Fc*CGT (mg/mL)	*Gm*SuSy (mg/mL)	Initial rate of mono-*C*-glucoside formation (mM/min)	Duration of first step[a] (min)	Initial rate of di-*C*-glucoside formation (mM/min)[a]	Final conversion to di-C-glucoside (%)	Ratio of UDP-Glc/UDP[b]	Ref.
1	10 mM phloretin	0.5	30	1.0	0.5	0.55	10–30	0.062	99 (6 h)	1.90	Figure 3
2	30 mM phloretin	0.5	30	2.0	1.0	0.17	<150	~0.015	71(19 h)	1.26	Supporting Information: Figure S7
3	30 mM phloretin	0.5	45	3.0	1.5	>1.0	<30	>0.30	99 (6 h)	0.97	Supporting Information: Figure S8
4	50 mM phloretin	0.5	45	3.0	1.5	0.19	<150	~0.14	71 (19 h)	0.97[c]	Supporting Information: Figure S9
5	50 mM phloretin	0.5	45	2.0 + 1.5[d]	1.0 + 0.8[d]	3.4	~60	0.059	76 (24 h)	0.98/0.66[e]	Supporting Information: Figure S10
6	50 mM phloretin	3.0	45	4.0	2.0	3.8	10–30	0.18	67 (24 h)	1.80	Supporting Information: Figure S11
7	50 mM phloretin	1.0	45	5.0	2.5	3.5	10–30	0.17	70 (24 h)	1.50	Supporting Information: Figure S12
8	50 mM phloretin	1.0	45	4.0	3.0	3.6	10–30	0.13	69 (24 h)	1.30	Supporting Information: Figure S13
9[f]	50 mM phloretin	1.0	45	4.0	2.0	3.8	10–30	0.18	69 (24 h)	1.20	Supporting Information: Figure S14
10	40 mM phloretin	1.0	45	6.0	3.0	>4.0	<10	0.44	99 (6 h)	1.20	Figure 4

TABLE 1 (Continued)

Entry	Substrate	UDP (mM)	Temp. (°C)	*Fc*CGT (mg/mL)	*Gm*SuSy (mg/mL)	Initial rate of mono-*C*-glucoside formation (mM/min)	Duration of first step[a] (min)	Initial rate of di-*C*-glucoside formation (mM/min)[a]	Final conversion to di-*C*-glucoside (%)	Ratio of UDP-Glc/UDP[b]	Ref.
11	30 mM PTHAP	0.5	45	3.0	1.5	>3.0	<10	0.57	99 (3 h)	1.70	Supporting Information: Figure S15
12	50 mM PTHAP	0.5	45	3.0	1.5	4.2	10–30	0.25	99 (24 h)	1.80	Figure 5

Abbreviation: PTHAP, 2-phenyl-2′,4′,6′-trihydroxyacetophenone.

[a]The initial rates were determined from the linear part of the time courses by multiplying the slope of the linear regression (%/min) with the substrate concentration (mM) giving the initial rate in mM/min.

[b]Concentrations of UDP and UDP-Glc at steady state were used for calculating the ratio.

[c]The ratio was calculated from the time point of 2.5 h.

[d]Enzymes were added by a two-step approach (first batch at the start, second batch at 4 h time point).

[e]The ratio of UDP-Glc and UDP changed from 0.98 to 0.66 after adding the second batch of catalysts.

[f]The pH was 7.0 (pH 6.5 for other entries).

re-established towards the end of the reaction requires consideration. At this point, UDP-Glc consumption by the *Fc*CGT reaction could no longer happen while a large surplus of sucrose was still available. HPLC analysis reveals the formation of decomposition products from UDP and UDP-Glc, in particular uridine and UMP, with time (Figure 5d). Inactivation of *Gm*SuSy and/or change in the reaction equilibrium due to conditions used (possible change in the pH during reaction, presence of PTHAP) could serve as plausible explanations for the unproductive regeneration of UDP-Glc at the end of the reaction.

3.5 | Synthesis and isolation of the di-*C*-glucosides of phloretin and PTHAP

Preparative reactions were performed at ~20 mg scale of synthesized di-*C*-glycoside product. Phloretin and PTHAP were used as the HPCD inclusion complex, each at 30 mM of the acceptor substrate in a total volume of 1.0 mL. Conversion of phloretin and PTHAP into the corresponding di-β-C-glucoside was monitored by HPLC and once it was complete (≥99%), the reaction mixture was frozen in liquid N_2 (Supporting Information: Figures S16 and S23). Development of an efficient procedure for the product isolation, here mostly for analytical characterization, was challenging for two reasons. One is the mixed polar-nonpolar (amphiphilic) character of the products. The other was product instability. The downstream processing of nothofagin developed in earlier work was not directly applicable due to product decomposition in the key anion exchange step. The anion exchange chromatographic purification of nothofagin was performed under basic pH of 8.5, to achieve ionization of the phenolic hydroxyl groups for allowing the separation from sucrose, fructose, and HPCD (Schmölzer et al., 2018). Phloretin-di-*C*-glucoside was largely decomposed in the anion exchange column under the conditions described for nothofagin (Supporting Information: Figure S17). We further attempted the separation by anion exchange chromatography at pH 4.3 to facilitate the stability of the target product, resulting in phloretin-di-*C*-glucoside not binding into the column resin and eluting in the flow through fraction. The flow through fraction with HPCD contamination was subjected to size-exclusion chromatographic purification as described for nothofagin, yet all the phloretin-*C*-glucoside decomposed at this point. Performing the size-exclusion chromatography with acidified water at pH 4.3 did not improve the product stability (Supporting Information: Figure S18). We then tested the purification of phloretin-3′,5′-di-*C*-β-glucoside via liquid–liquid extraction with different organic solvents: 1-butanol, 1-octanol, ethyl acetate, diethyl ether, and dichloromethane (Supporting Information: Figure S19A). The extraction with 1-butanol gave the di-*C*-glucoside mainly in the organic phase, yet with a significant contamination from fructose, sucrose, and HPCD (Supporting Information: Figure S19A). Considering the low solubility of HPCD in acetone, the organic phases from up-scaled (0.70 mL instead of 0.08 mL reaction mixture) 1-butanol extraction were evaporated to

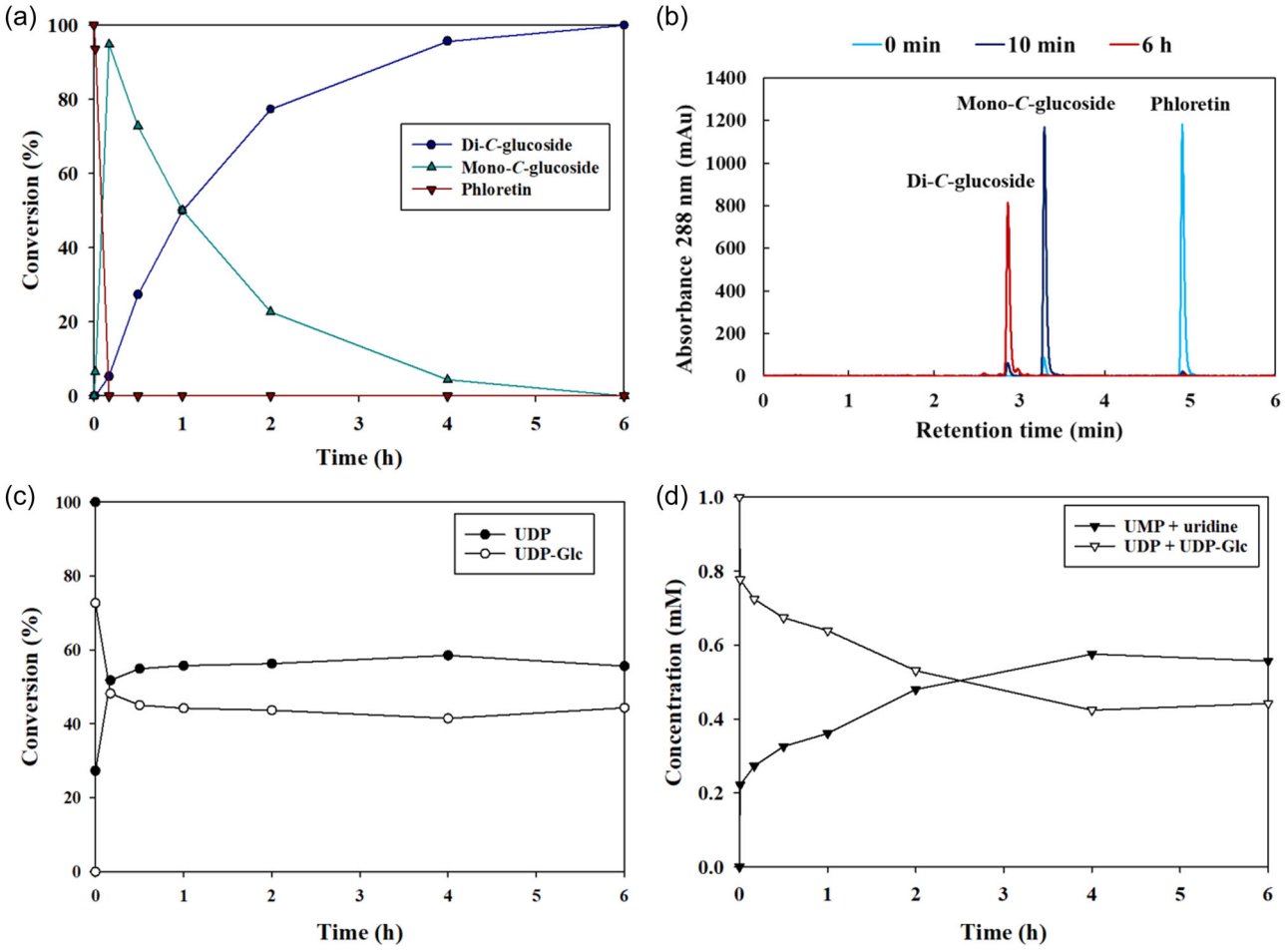

FIGURE 4 Enzyme cascade transformation for di-*C*-glycosylation of phloretin (40 mM; HPCD complex) performed at 45°C. (a) Time course for phloretin (red triangles), nothofagin (blue circles), and phloretin-3′,5′-di-C-β-glucoside (cyan triangles). (b) Overlay of reverse phase HPLC chromatograms from the reaction at 0 min (light blue), 10 min (dark blue), and 6 h (red). (c) Time course for UDP (closed circles) and UDP-Glc (open circles). (d) Time course for the summed-up concentrations (mM) of UDP and UDP-Glc (open triangles) and decomposition products uridine and UMP (closed triangles). The amount of UDP supplied was 1.0 mM. HPCD, 2-hydroxypropyl-β-cyclodextrin; UDP, uridine-5′-diphosphate; UDP-Glc, UDP-glucose.

dryness and re-dissolved in acetone with the aim of increasing the purity of the desired product. Phloretin-di-*C*-glucoside was not found in the acetone extracts, yet it could be identified (together with sucrose, fructose, and HPCD) on TLC when the crystals from 1-butanol extraction were further dissolved in water (Supporting Information: Figure S19B).

While evaluating different purification methods, we found that standard TLC on silica plates, using 1-butanol/acetic acid/deionized water (2:1:1) as the mobile phase, achieved efficient separation of the phloretin-3′,5′-di-C-β-glucoside from the bulk of carbohydrates (sucrose, fructose, HPCD) present in the reaction mixture. About 21.6 mg product (1.2 mL mixture) were processed in a single run of preparative TLC (Supporting Information: Figure S20). After collection from the plate and extraction with acetone, the di-*C*-glycoside was recovered in excellent purity (≥95%; HPLC; Supporting Information: Figure S21) in ~80% yield. NMR data (Supporting Information: Figure S22) confirmed the identity as phloretin-3′,5′-di-C-β-glucoside.

Attempts to obtain the PTHAP-3′,5′-di-C-β-glucoside by analogous procedure of preparative TLC were unsuccessful due to complete decomposition of the product while re-extracting it from the silica gel. Using column chromatography on a silica C18 resin, the di-*C*-glycoside was eluted together with the HPCD. Re-chromatography of the concentrated product fractions on the same C18 column did not yield the di-*C*-glycoside in sufficient purity (data not shown). Isolation of the PTHAP-3′,5′-di-C-β-glucoside was eventually accomplished by a combination of C18 and silica 60 columns. The silica 60 column operated with the TLC eluent as the mobile phase succeeded in separating the PTHAP-3′,5′-di-C-β-glucoside from the other compounds, but it also led to a silica contamination. The C18 column operated with water was used to wash out the dissolved silica. The target compound was eluted with acetonitrile. The explorative purification procedure here used gave

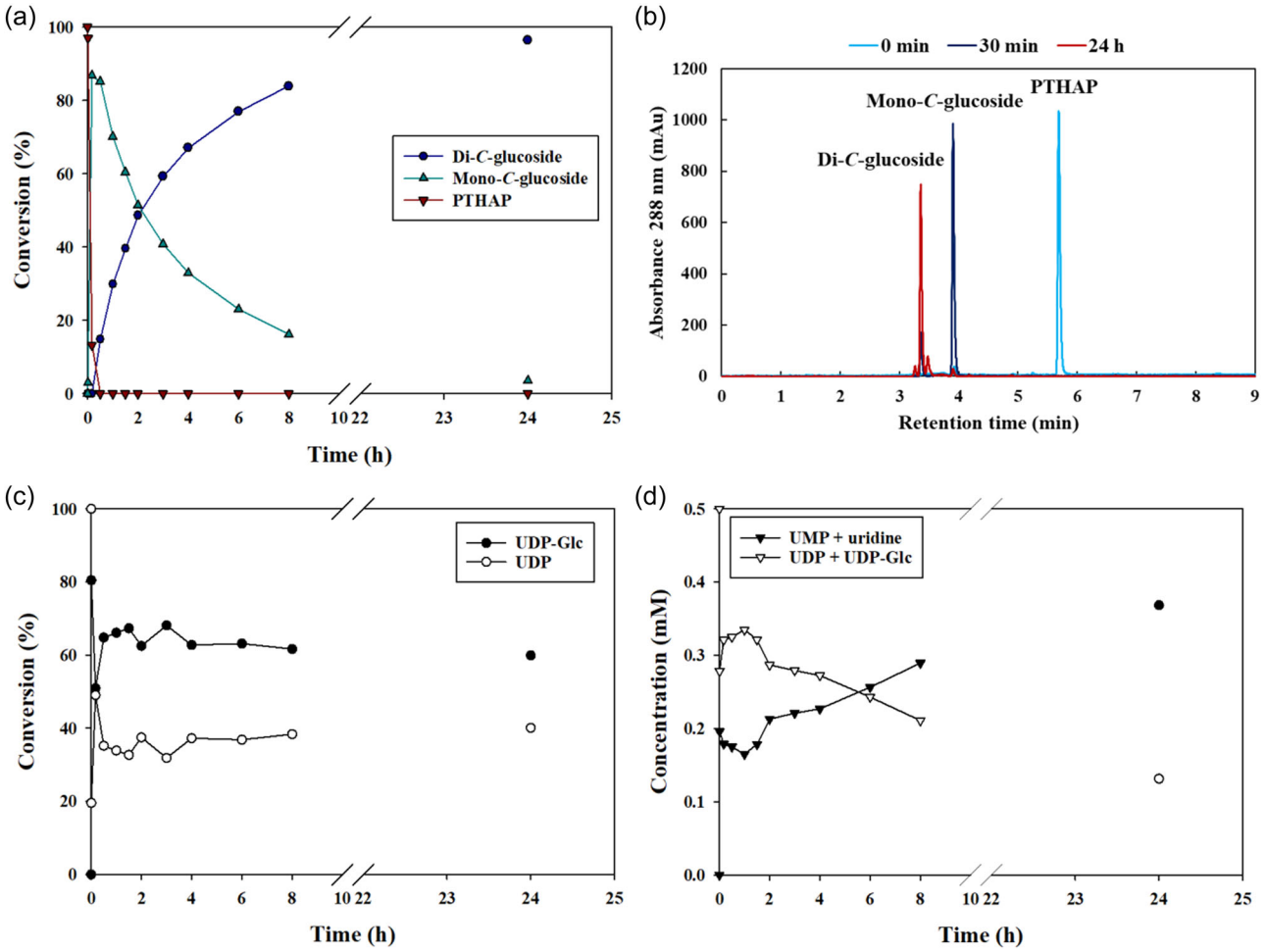

FIGURE 5 Enzyme cascade transformation for di-C-glycosylation of PTHAP (50 mM; HPCD complex). (a) Time course for PTHAP (red triangles), PTHAP-mono-C-glucoside (blue circles) and PTHAP-3′,5′-di-C-β-glucoside (cyan triangles). (b) Overlay of reverse phase HPLC chromatograms from the reaction at 0 min (light blue), 30 min (dark blue), and 24 h (red). (c) Time course for UDP (open circles) and UDP-Glc (closed circles). (d) Time course for the summed-up concentrations (mM) of UDP and UDP-Glc (open triangles) and decomposition products uridine and UMP (closed triangles). The amount of UDP supplied was 0.5 mM. HPCD, 2-hydroxypropyl-β-cyclodextrin; PTHAP, 2-phenyl-2′, 4′,6′-trihydroxyacetophenone; UDP, uridine-5′-diphosphate; UDP-Glc, UDP-glucose.

the authentic PTHAP-3′,5′-di-C-β-glucoside (NMR data in Supporting Information: Figure S25) in high purity (≥95%, HPLC data in Supporting Information: Figure S24), thus fulfilling the basic requirements for follow-up applications. The product yield (4.9 mg; ~20%) is considered preliminary at this point, due to the number of purification steps applied. A streamlined procedure would involve two-column chromatographic steps only, silica 60 first, C18 afterwards.

Lastly, we performed a preliminary investigation on the spontaneous decomposition of the di-C-β-glucoside products. The isolated phloretin-3′,5′-di-C-β-glucoside was analyzed in incubations at pH 8.0 (2.0 mM; 1.0 mL in water). Extensive set of HPLC-UV/MS data suggests degradation into multiple species apparently bearing a multihydroxylated aromatic core structure (Supporting Information: Figures S26 and S27). Degradation seems to involve loss of the two glucose residues from the aromatic core in ways that must await further study for clarification.

4 | CONCLUSIONS

Process intensification for biocatalytic production of the 3′,5′-di-C-β-glucosides of phloretin and PTHAP, representing phenolic aglycones from the natural products and synthetic chemical classes of compounds required reaction engineering at three levels. First, the aglycone solubility was enhanced by inclusion complexation in HPCD. The strategy was demonstrated in earlier work for the biocatalytic mono-C-glycosylation of phloretin to give nothofagin (H. Liu & Nidetzky, 2021; H. Liu et al., 2021; Schmölzer et al., 2018), but its applicability to the di-glycosylation of aglycones was not shown before. Second, prevention of di-C-β-glucoside decomposition by oxidative chemical processes was essential for efficient and selective bioproduction. The high reactivity of the di-C-β-glucosides was implied by prior works on the characterization of these compounds as antioxidants and other pharmacological agents (Kanamori et al., 2018; Mannem et al., 2020; Marrelli et al., 2014;

Materska, 2014; Wen et al., 2017; Xiao et al., 2014; Xie et al., 2020), but the pronounced requirement for stabilization even in the enzymatic synthesis was unexpected and new. Third, biocatalytic production at high yield (≥95%), concentration (30–50 mM), and space–time yield (~10 mM/h) necessitated an optimization of the reaction conditions, regarding the amount of enzyme used and avoidance of substrate inhibition. Overall, the intensification achieved on the product concentration metric of the process performance was between 30- and 150-fold compared to earlier studies that were limited in the acceptor concentrations used (0.2–1.5 mM). Moreover, enzymatic di-*C*-glycosylation under use of sucrose synthase for provision of UDP-Glc in situ from sucrose was shown for the first time. A preliminary account of product recovery from the reaction mixtures was presented and the chemical identity of the 3′,5′-di-*C*-β-glucosides of phloretin and PTHAP was confirmed. Overall, therefore, we show efficient GT cascade reaction for flexible use in natural product di-*C*-β-glucoside synthesis from expedient substrates. Demonstrating the enzymatic reactions at a larger scale than shown here can be an important task for future studies.

AUTHOR CONTRIBUTIONS

Tuo Li, **Annika J. E. Borg**, and **Bernd Nidetzky**: Design of study. **Tuo Li** and **Annika J. E. Borg**: All experiments. **Tuo Li**, **Annika J. E. Borg**, and **Leo Krammer**: Product isolation. **Rolf Breinbauer**: Supervision and resources. **Tuo Li**, **Annika J. E. Borg**, and **Bernd Nidetzky**: Manuscript writing. **Bernd Nidetzky**: Funding acquisition.

ACKNOWLEDGMENTS

The COMET center acib: Next Generation Bioproduction is funded by BMK, BMDW, SFG, Standortagentur Tirol, Government of Lower Austria und Vienna Business Agency in the framework of COMET—Competence Centers for Excellent Technologies. The COMET-Funding Program is managed by the Austrian Research Promotion Agency FFG.

CONFLICT OF INTEREST STATEMENT

The authors declare no conflict of interest.

DATA AVAILABILITY STATEMENT

The data that support the findings of this study are available from the corresponding author upon reasonable request.

ORCID

Annika J. E. Borg https://orcid.org/0000-0003-1311-6910
Leo Krammer https://orcid.org/0000-0002-4861-754X
Rolf Breinbauer https://orcid.org/0000-0001-6009-7359
Bernd Nidetzky http://orcid.org/0000-0002-5030-2643

REFERENCES

Abbas, M., Saeed, F., Anjum, F. M., Afzaal, M., Tufail, T., Bashir, M. S., Ishtiaq, A., Hussain, S., & Suleria, H. A. R. (2016). Natural polyphenols: An overview. *International Journal of Food Properties*, *20*, 1689–1699. https://doi.org/10.1080/10942912.2016.1220393

Bao, Y. O., Zhang, M., Qiao, X., & Ye, M. (2022). Functional characterization of a C-glycosyltransferase from *Pueraria lobata* with dual-substrate selectivity. *Chemical Communications*, *58*, 12337–12340. https://doi.org/10.1039/d2cc04279g

Behzad, S., Sureda, A., Barreca, D., Nabavi, S. F., Rastrelli, L., & Nabavi, S. M. (2017). Health effects of phloretin: From chemistry to medicine. *Phytochemistry Reviews*, *16*, 527–533. https://doi.org/10.1007/s11101-017-9500-x

Cesari, A., Uccello Barretta, G., Kirschner, K. N., Pappalardo, M., Basile, L., Guccione, S., Russotto, C., Lauro, M. R., Cavaliere, F., & Balzano, F. (2020). Interaction of natural flavonoid eriocitrin with β-cyclodextrin and hydroxypropyl-β-cyclodextrin: An NMR and molecular dynamics investigation. *New Journal of Chemistry*, *44*, 16431–16441. https://doi.org/10.1039/d0nj02022b

Chen, D., Chen, R., Xie, K., Duan, Y., & Dai, J. (2018). Production of acetophenone C-glucosides using an engineered C-glycosyltransferase in *Escherichia coli*. *Tetrahedron Letters*, *59*, 1875–1878. https://doi.org/10.1016/j.tetlet.2018.04.006

Chen, D., Fan, S., Chen, R., Xie, K., Yin, S., Sun, L., Liu, J., Yang, L., Kong, J., Yang, Z., & Dai, J. (2018). Probing and engineering key residues for bis-C-glycosylation and promiscuity of a C-glycosyltransferase. *ACS Catalysis*, *8*, 4917–4927. https://doi.org/10.1021/acscatal.8b00376

Chong, Y., Lee, S. W., & Ahn, J. H. (2022). Phenolic C-glycoside synthesis using microbial systems. *Current Opinion in Biotechnology*, *78*, 102827. https://doi.org/10.1016/j.copbio.2022.102827

Dai, L., Hu, Y., Chen, C. C., Ma, L., & Guo, R. T. (2021). Flavonoid C-glycosyltransferases: Function, evolutionary relationship, catalytic mechanism and protein engineering. *ChemBioEng Reviews*, *8*, 15–26. https://doi.org/10.1002/cben.202000009

Durazzo, A., Lucarini, M., Souto, E. B., Cicala, C., Caiazzo, E., Izzo, A. A., Novellino, E., & Santini, A. (2019). Polyphenols: A concise overview on the chemistry, occurrence, and human health. *Phytotherapy Research*, *33*, 2221–2243. https://doi.org/10.1002/ptr.6419

Fang, Z., & Bhandari, B. (2010). Encapsulation of polyphenols—A review. *Trends in Food Science & Technology*, *21*, 510–523. https://doi.org/10.1016/j.tifs.2010.08.003

Feng, C. Y., Li, S. S., Taguchi, G., Wu, Q., Yin, D. D., Gu, Z. Y., Wu, J., Xu, W. Z., Liu, C., & Wang, L. S. (2021). Enzymatic basis for stepwise C-glycosylation in the formation of flavonoid di-C-glycosides in sacred lotus (*Nelumbo nucifera Gaertn.*). *The Plant Journal*, *106*, 351–365. https://doi.org/10.1111/tpj.15168

Gao, H. Y., Liu, Y., Tan, F. F., Zhu, L. W., Jia, K. Z., & Tang, Y. J. (2022). The advances and challenges in enzymatic C-glycosylation of flavonoids in plants. *Current Pharmaceutical Design*, *28*, 1466–1479. https://doi.org/10.2174/1381612828666220422085128

Gratieri, T., Pinho, L. A. G., Oliveira, M. A., Sa-Barreto, L. L., Marreto, R. N., Silva, I. C., Gelfuso, G. M., de Souza Siqueira Quintans, J., Quintans-Junior, L. J., & Cunha-Filho, M. (2020). Hydroxypropyl-β-cyclodextrin-complexed naringenin by solvent change precipitation for improving anti-inflammatory effect in vivo. *Carbohydrate Polymers*, *231*, 115769. https://doi.org/10.1016/j.carbpol.2019.115769

He, B., Bai, X., Tan, Y., Xie, W., Feng, Y., & Yang, G. Y. (2022). Glycosyltransferases: Mining, engineering and applications in biosynthesis of glycosylated plant natural products. *Synthetic and Systems Biotechnology*, *7*, 602–620. https://doi.org/10.1016/j.synbio.2022.01.001

Huang, J., She, Y., Yue, J., Chen, Y., Li, Y., Li, J., Hu, Y., Yang, D., Chen, J., Yang, L., Liu, Z., Wu, R., Jin, P., & Duan, L. (2022). Exploring the catalytic function and active sites of a novel C-glycosyltransferase from *Anemarrhena asphodeloides*. *Synthetic and Systems Biotechnology*, *7*, 621–630. https://doi.org/10.1016/j.synbio.2022.01.003

Ito, T., Fujimoto, S., Suito, F., Shimosaka, M., & Taguchi, G. (2017). C-Glycosyltransferases catalyzing the formation of di-C-glucosyl flavonoids in citrus plants. *The Plant Journal*, *91*, 187–198. https://doi.org/10.1111/tpj.13555

Kanamori, T., Matsuyama, A., Naito, H., Tsuga, Y., Ozako, Y., Ogura, S., Okazaki, S., & Yuasa, H. (2018). Water-soluble glucosyl pyrene

photosensitizers: An intramolecularly synthesized 2- C-glucoside and an O-glucoside. *The Journal of Organic Chemistry*, *83*, 13765–13775. https://doi.org/10.1021/acs.joc.8b02066

Kaur, H., & Kaur, G. (2014). A critical appraisal of solubility enhancement techniques of polyphenols. *Journal of Pharmaceutics*, *2014*, 180845. https://doi.org/10.1155/2014/180845

Kellici, T. F., Chatziathanasiadou, M. V., Diamantis, D., Chatzikonstantinou, A. V., Andreadelis, I., Christodoulou, E., Valsami, G., Mavromoustakos, T., & Tzakos, A. G. (2016). Mapping the interactions and bioactivity of quercetin-(2-hydroxypropyl)-β-cyclodextrin complex. *International Journal of Pharmaceutics*, *511*, 303–311. https://doi.org/10.1016/j.ijpharm.2016.07.008

Kitamura, K., Ando, Y., Matsumoto, T., & Suzuki, K. (2018). Total synthesis of aryl C-glycoside natural products: Strategies and tactics. *Chemical Reviews*, *118*, 1495–1598. https://doi.org/10.1021/acs.chemrev.7b00380

Lemmerer, M., Schmölzer, K., Gutmann, A., & Nidetzky, B. (2016). Downstream processing of nucleoside-diphospho-sugars from sucrose synthase reaction mixtures at decreased solvent consumption. *Advanced Synthesis & Catalysis*, *358*, 3113–3122. https://doi.org/10.1002/adsc.201600540

Li, X., Meng, X., de Leeuw, T. C., Te Poele, E. M., Pijning, T., Dijkhuizen, L., & Liu, W. (2021). Enzymatic glucosylation of polyphenols using glucansucrases and branching sucrases of glycoside hydrolase family 70. *Critical Reviews in Food Science and Nutrition*, 1–21. https://doi.org/10.1080/10408398.2021.2016598

Liu, C. F. (2022). Recent advances on natural aryl-C-glycoside scaffolds: Structure, bioactivities, and synthesis—A comprehensive review. *Molecules*, *27*, 7439. https://doi.org/10.3390/molecules27217439

Liu, H., & Nidetzky, B. (2021). Leloir glycosyltransferases enabled to flow synthesis: Continuous production of the natural C-glycoside nothofagin. *Biotechnology and Bioengineering*, *118*, 4402–4413. https://doi.org/10.1002/bit.27908

Liu, H., Tegl, G., & Nidetzky, B. (2021). Glycosyltransferase co-immobilization for natural product glycosylation: Cascade biosynthesis of the C-glucoside nothofagin with efficient reuse of enzymes. *Advanced Synthesis & Catalysis*, *363*, 2157–2169. https://doi.org/10.1002/adsc.202001549

Luo, J., Si, H., Jia, Z., & Liu, D. (2021). Dietary anti-aging polyphenols and potential mechanisms. *Antioxidants*, *10*, 283. https://doi.org/10.3390/antiox10020283

Mannem, R. R., Thoti, N., & Aidhen, I. S. (2020). Bioactive C-glycosides inspired from natural products towards therapeutics. In V. K. Tiwari (Ed.), *Carbohydrates in drug discovery and development* (pp. 97–153). Elsevier.

Marrelli, M., Menichini, G., Provenzano, E., & Conforti, F. (2014). Applications of natural compounds in the photodynamic therapy of skin cancer. *Current Medicinal Chemistry*, *21*, 1371–1390. https://doi.org/10.2174/09298673211214031909432 4

Materska, M. (2014). Flavone C-glycosides from *Capsicum annuum L.*: Relationships between antioxidant activity and lipophilicity. *European Food Research and Technology*, *240*, 549–557. https://doi.org/10.1007/s00217-014-2353-2

Mithul Aravind, S., Wichienchot, S., Tsao, R., Ramakrishnan, S., & Chakkaravarthi, S. (2021). Role of dietary polyphenols on gut microbiota, their metabolites and health benefits. *Food Research International*, *142*, 110189. https://doi.org/10.1016/j.foodres.2021.110189

Oualid, O., & M. S. Silva, A. (2012). Advances in C-glycosylflavonoid research. *Current Organic Chemistry*, *16*, 859–896. https://doi.org/10.2174/138527212800194791

Putkaradze, N., Teze, D., Fredslund, F., & Welner, D. H. (2021). Natural product C-glycosyltransferases—A scarcely characterised enzymatic activity with biotechnological potential. *Natural Product Reports*, *38*, 432–443. https://doi.org/10.1039/d0np00040j

Rasouli, H., Farzaei, M. H., & Khodarahmi, R. (2017). Polyphenols and their benefits: A review. *International Journal of Food Properties*, *20*, 1700–1741. https://doi.org/10.1080/10942912.2017.1354017

Ren, Z., Ji, X., Jiao, Z., Luo, Y., Zhang, G. Q., Tao, S., Lei, Z., Zhang, J., Wang, Y., Liu, Z. J., & Wei, G. (2020). Functional analysis of a novel C-glycosyltransferase in the orchid *Dendrobium catenatum*. *Horticulture Research*, *7*, 111. https://doi.org/10.1038/s41438-020-0330-4

Sato, S., Nojiri, T., Okuyama, N., Maeda, K., & Kirigane, A. (2020). Synthesis and evaluation of a new water-soluble fluorescent red dye, xanthene bis-C-glycoside. *Journal of Heterocyclic Chemistry*, *57*, 3342–3349. https://doi.org/10.1002/jhet.4050

Schmölzer, K., Lemmerer, M., & Nidetzky, B. (2018). Glycosyltransferase cascades made fit for chemical production: Integrated biocatalytic process for the natural polyphenol C-glucoside nothofagin. *Biotechnology and Bioengineering*, *115*, 545–556. https://doi.org/10.1002/bit.26491

Shakoor, H., Feehan, J., Apostolopoulos, V., Platat, C., Al Dhaheri, A. S., Ali, H. I., Ismail, L. C., Bosevski, M., & Stojanovska, L. (2021). Immunomodulatory effects of dietary polyphenols. *Nutrients*, *13*, 728. https://doi.org/10.3390/nu13030728

Shie, J. J., Chen, C. A., Lin, C. C., Ku, A. F., Cheng, T. J. R., Fang, J. M., & Wong, C. H. (2010). Regioselective synthesis of di-C-glycosylflavones possessing anti-inflammation activities. *Organic & Biomolecular Chemistry*, *8*, 4451–4462. https://doi.org/10.1039/c0ob00011f

Sun, C., Zhao, C., Guven, E. C., Paoli, P., Simal-Gandara, J., Ramkumar, K. M., Wang, S., Buleu, F., Pah, A., Turi, V., Damian, G., Dragan, S., Tomas, M., Khan, W., Wang, M., Delmas, D., Portillo, M. P., Dar, P., Chen, L., & Xiao, J. (2020). Dietary polyphenols as antidiabetic agents: Advances and opportunities. *Food Frontiers*, *1*, 18–44. https://doi.org/10.1002/fft2.15

Sun, Y., Chen, Z., Yang, J., Mutanda, I., Li, S., Zhang, Q., Zhang, Y., Zhang, Y., & Wang, Y. (2020). Pathway-specific enzymes from bamboo and crop leaves biosynthesize anti-nociceptive C-glycosylated flavones. *Communications Biology*, *3*, 110. https://doi.org/10.1038/s42003-020-0834-3

Tegl, G., & Nidetzky, B. (2020). Leloir glycosyltransferases of natural product C-glycosylation: Structure, mechanism and specificity. *Biochemical Society Transactions*, *48*, 1583–1598. https://doi.org/10.1042/BST20191140

Teze, D., Bidart, G. N., & Welner, D. H. (2022). Family 1 glycosyltransferases (GT1, UGTs) are subject to dilution-induced inactivation and low chemo stability toward their own acceptor substrates. *Frontiers in Molecular Biosciences*, *9*, 909659. https://doi.org/10.3389/fmolb.2022.909659

Thuan, N. H., & Sohng, J. K. (2013). Recent biotechnological progress in enzymatic synthesis of glycosides. *Journal of Industrial Microbiology and Biotechnology*, *40*, 1329–1356. https://doi.org/10.1007/s10295-013-1332-0

Wang, Z., He, Y., Liao, L., Zhang, Y., Zhao, Y., Xiao, Y., Jiang, X., & Qiao, F. (2022). Forming coumarin C-glycosides via biocatalysis: Characterization of a C-glycosyltransferase from *Angelica decursiva*. *Biochemical and Biophysical Research Communications*, *614*, 85–91. https://doi.org/10.1016/j.bbrc.2022.05.008

Wang, Z. L., Gao, H. M., Wang, S., Zhang, M., Chen, K., Zhang, Y. Q., Wang, H. D., Han, B. Y., Xu, L. L., Song, T. Q., Yun, C. H., Qiao, X., & Ye, M. (2020). Dissection of the general two-step di-C-glycosylation pathway for the biosynthesis of (iso)schaftosides in higher plants. *Proceedings of the National Academy of Sciences*, *117*, 30816–30823. https://doi.org/10.1073/pnas.2012745117

Wen, L., Zhao, Y., Jiang, Y., Yu, L., Zeng, X., Yang, J., Tian, M., Liu, H., & Yang, B. (2017). Identification of a flavonoid C-glycoside as potent antioxidant. *Free Radical Biology and Medicine*, *110*, 92–101. https://doi.org/10.1016/j.freeradbiomed.2017.05.027

Xiao, J. (2015). Dietary flavonoid aglycones and their glycosides: Which show better biological significance? *Critical Reviews in Food Science and Nutrition*, *57*, 1874–1905. https://doi.org/10.1080/10408398.2015.1032400

Xiao, J., Capanoglu, E., Jassbi, A. R., & Miron, A. (2016). Advance on the flavonoid C-glycosides and health benefits. *Critical Reviews in Food Science and Nutrition*, *56*, 29–45. https://doi.org/10.1080/10408398.2015.1067595

Xiao, J., Muzashvili, T. S., & Georgiev, M. I. (2014). Advances in the biotechnological glycosylation of valuable flavonoids. *Biotechnology Advances*, *32*, 1145–1156. https://doi.org/10.1016/j.biotechadv.2014.04.006

Xie, K., Zhang, X., Sui, S., Ye, F., & Dai, J. (2020). Exploring and applying the substrate promiscuity of a C-glycosyltransferase in the chemo-enzymatic synthesis of bioactive C-glycosides. *Nature Communications*, *11*, 5162. https://doi.org/10.1038/s41467-020-18990-9

Zeng, P., Zhang, Y., Pan, C., Jia, Q., Guo, F., Li, Y., Zhu, W., & Chen, K. (2013). Advances in studying of the pharmacological activities and structure–activity relationships of natural C-glycosylflavonoids. *Acta Pharmaceutica Sinica B*, *3*, 154–162. https://doi.org/10.1016/j.apsb.2013.04.004

Zhang, M., Li, F. D., Li, K., Wang, Z. L., Wang, Y. X., He, J. B., Su, H. F., Zhang, Z. Y., Chi, C. B., Shi, X. M., Yun, C. H., Zhang, Z. Y., Liu, Z. M., Zhang, L. R., Yang, D. H., Ma, M., Qiao, X., & Ye, M. (2020). Functional characterization and structural basis of an efficient di-C-glycosyltransferase from *Glycyrrhiza glabra*. *Journal of the American Chemical Society*, *142*, 3506–3512. https://doi.org/10.1021/jacs.9b12211

Zhang, Y. Q., Zhang, M., Wang, Z. L., Qiao, X., & Ye, M. (2022). Advances in plant-derived C-glycosides: Phytochemistry, bioactivities, and biotechnological production. *Biotechnology Advances*, *60*, 108030. https://doi.org/10.1016/j.biotechadv.2022.108030

Zheng, Y., Haworth, I. S., Zuo, Z., Chow, M. S. S., & Chow, A. H. L. (2005). Physicochemical and structural characterization of Quercetin-β-Cyclodextrin complexes. *Journal of Pharmaceutical Sciences*, *94*, 1079–1089. https://doi.org/10.1002/jps.20325

SUPPORTING INFORMATION

Additional supporting information can be found online in the Supporting Information section at the end of this article.

How to cite this article: Li, T., Borg, A. J. E., Krammer, L., Breinbauer, R., & Nidetzky, B. (2023). Reaction intensification for biocatalytic production of polyphenolic natural product di-*C*-β-glucosides. *Biotechnology and Bioengineering*, 120, 1506–1520. https://doi.org/10.1002/bit.28354